Effect of loudspeaker non-linearities on the of personal sound zones

Loris Habib, Manuel Melon

forum acusticum 2023

EFFECT OF LOUDSPEAKER NON-LINEARITIES ON THE PERFORMANCE OF PERSONAL SOUND ZONES

Loris Habib **Manuel Melon***
Laboratoire d'Acoustique de l'Université du Mans (LAUM), UMR 6613,
Institut d'Acoustique - Graduate School (IA-GS), CNRS, 72000 Le Mans Université, France

ABSTRACT

Personal sound zones (PSZ) allow several people sharing the same room to listen to different audio content without using headphones. Loudspeaker arrays with filtered inputs are typically used to create the PSZ. The driving filters are calculated from the transfer functions between each loudspeaker and the points sampling each listening zone. These filters are usually computed once and are no longer relevant if the loudspeakers are driven at higher levels, especially for low-cost drivers which can exhibit a strong non-linear behavior. In this paper, a state space model is used to predict the nonlinear behavior of loudspeakers. Nonlinear parameters (force factor, stiffness and inductance) as a function of the diaphragm displacement are measured for each 2" Tectonic loudspeaker using a Klippel R&D system. Then, the accuracy of the state space model is checked by comparing the predicted harmonic distortion to the measured one for several input levels. Finally, the state-space representation is used to predict the effect of non-linearities on PSZ metrics. Simulation results show that the contrast can be reduced by about 10 dB and the error can increase by a factor of about 1000 in the low frequency range when large input signals are required.

Keywords: *loudspeaker arrays, sound zones, non-linearities.*

**Corresponding author*: *manuel.melon@univ-lemans.fr.*

1. INTRODUCTION

Personal sound zone (PSZ) systems allow listeners in the same room to enjoy different audio programs without using headphones. Sound zones are defined where it is desired to constrain the sound field, the rest of the volume of the listening room is usually not considered. The objective is then to attenuate the sound level in the other zone(s) when an audio signal is played in a given zone. One of the most common solutions is to use a speaker array whose input signals have been filtered to provide the expected separation of audio programs. The filter weights are generally computed using a constraint optimization method that allows to meet several criteria. For example, the potential energy of the sound in the different zones can be bounded to provide a sound level contrast between them. The input power of the speakers can also be penalized to protect them from damage or even the phase of the reproduced signal to achieve a natural localization of the reproduced sound sources.

Since the work of Druyvesteyn and Garas [1], PSZs have been widely studied and several algorithms have been proposed. Among the most used ones, we can cite the Acoustic Contrast Control (ACC) method [2, 3] or the Pressure Matching (PM) algorithm [4].

For these methods, the sound zone filters are calculated from the transfer functions between the loudspeakers and points sampling the listening zones. Given the complexity of the spaces we live in, these transfer functions are often measured rather than simulated in order to obtain sufficient accuracy. The transfer functions are measured at a given input level, but the loudspeakers can then be driven at another level, sometimes much higher. Either because one wishes to modify the listening level, or because the creation of the sound zones requires it. Unfor-

tunately, loudspeakers exhibit non-linear behavior when used at high input levels [5]. As a result, filters calculated from measurements made at a given level can have their performance downgraded when the loudspeakers are used at higher levels.

Such behaviour has already been studied by Ma *et al.* [6,7] for the ACC algorithm by modelling the loudspeaker non-linear distortion using a simplified Volterra-like model. In the work proposed here, the effect of speaker non-linearities on the performance of the PM algorithm is studied in the context of a state-space formalism. This approach can provide a better understanding of the physical causes of PSZ performance loss.

In this article, Section 2 introduces the modelling of the non-linear loudspeaker behaviour using a state space model. Measurement results are also provided to assess the model accuracy. Section 3 presents the sound zone algorithm used in this work. Simulation results of a simplified sound zone scenario are provided in Section 4 to investigate the effect of loudspeaker non-linearities on the performance of the sound zone algorithm. Finally, the article concludes by recalling the main results and proposing future work.

2. SPEAKER MODELLING

Electrodynamic loudspeakers are often modelled in the linear domain by using the Thiele & Small model [8, 9]. However, for large excitation signals, such drivers exhibit a non-linear behaviour that can be modelled using a state-space representation [10, 11]

$$\dot{\mathbf{x}} = \mathbf{A}\mathbf{x} + \mathbf{B}U, \tag{1}$$

where $\mathbf{u}$ is the input vector and $\mathbf{x}$ is the state space vector. The matrix $\mathbf{A}$ and the vector $\mathbf{B}$ describe the non-linear behaviour of the loudspeaker. The root causes of non-linearities of electrodynamic drivers are very diverse [5]. In this work, it was chosen to model the most impacting ones by taking into account the dependence of the force factor Bl, the suspension compliance C_{ms} and the voice coil inductance with the diaphragm position $x(t)$.

The non-linear Lumped Element Model (LEM) used in this paper is presented in Fig. 1. In this circuit, U is the driving voltage. R_e and L_e respectively are the resistor and inductor parts of the voice coil. R_{ms} and M_{ms} respectively are the mechanical resistance and mass of the voice coil-diaphragm assembly. C_{mc} represents the compliance of the loudspeaker mounted in a closed box. An additional reluctance force $F_m(x, i)$ due to the variation

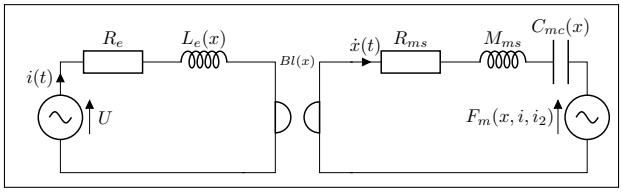

Figure 1. Equivalent circuit of the closed box speaker.

of L_e with the displacement is also introduced [5], it is approximated with

$$F_m(x, i) = -\frac{i^2(t)}{2}\frac{\partial L_e(x)}{\partial x}, \tag{2}$$

where current $i(t)$ is flowing in the inductor L_e.

Considering the LEM model used here, the input vector $\mathbf{x}$ is given by

$$\mathbf{x} = [x(t), \dot{x}(t), i(t)]^T, \tag{3}$$

where the superscript ^{T} denotes the transpose operation and the overscript $\dot{}$ represents the time derivative. Matrix A is then given in Eq. 5 while $\mathbf{B}$ is equal to

$$\mathbf{B} = \left[0, 0, \frac{1}{L_e}\right]^T. \tag{4}$$

The state space model of Eq. 1 is solved using the following discrete form:

$$\mathbf{x}(n+1) = \mathbf{A_d}\mathbf{x}(n) + \mathbf{B_d}\mathbf{u}(n), \tag{6}$$

by using a bilinear transform for which

$$\mathbf{A_d} = \left(\mathbf{I} - \frac{\mathbf{A}T_s}{2}\right)^{-1}\left(\mathbf{I} + \frac{\mathbf{A}T_s}{2}\right), \tag{7}$$

$$\mathbf{B_d} = \left(\mathbf{I} - \frac{\mathbf{A}T_s}{2}\right)^{-1}\mathbf{B}T_s, \tag{8}$$

where T_s is the timestep. The values of the matrix $\mathbf{A}$ involving entries of the vector $\mathbf{x}$ are taken equal to their values at discrete time n in order to calculate $\mathbf{x}(n+1)$. The values of the voice coil position-dependent parameters at $n+1$ are calculated from the value of $x(n)$ and measurements giving the variation of these parameters as a function of position for the speaker considered.

The dependencies of the Bl factor, compliance C_{mc} and inductance L_e with the displacement amplitude have been measured using a Klippel R&D system for the 8 Tectonic TEBM46C20N loudspeakers used in this work. The

$$A = \begin{bmatrix} 0 & 1 & 0 \\ -\dfrac{1}{M_{ms}C_{mc}(x)} & -\dfrac{R_{ms}}{M_{ms}} & \dfrac{Bl(x) + \frac{1}{2}\frac{\partial L_e(x)}{\partial x} i(t)}{M_{ms}} \\ 0 & -\dfrac{Bl(x) + \frac{\partial L_e(x)}{\partial x} i(t)}{L_e(x)} & -\dfrac{R_e}{L_e(x)} \end{bmatrix} \tag{5}$$

curves for one of these units are shown in Fig. 2 for the following range of displacement: $|x| \leq 3$ mm. For large displacements the voice coil moves in and out of the air gap which results in a smaller portion of the coil that is affected by the magnetic field. Consequently, the Bl factor gets lower as the position increases or decreases as seen in Fig. 2. We notice that the value of Bl decreases by about 45% for $|x| = 3$ mm. The Bl curve shows an almost symmetrical behaviour, although its maximum is obtained at $x = 0.2$ mm. It is therefore common to observe such an asymmetric behaviour, which results in even order harmonics and a DC offset.

The compliance C_{mc} has a similar shape than the Bl factor, it decreases by about 40% for $|x| = 3$ mm. Indeed, for large excitation levels, the suspension materials are stretched increasingly and thus becomes stiffer, which limits the displacement of the diaphragm.

The inductance L_e has an asymmetrical behaviour, with a value that increases when the voice coil is moved into the air gap. As the amount of the coil in the air gap changes with the displacement, the magnetic flux seen by the coil also changes. As a result, the apparent inductance increases or decreases, and this variation depends on the permeability of the surrounding parts. For inward movement, the coil is mainly surrounded by parts with high permeability, so the apparent inductance increases.

In order to evaluate the validity of the proposed model, measurements of the frequency response in the nearfield of the Tectonic loudspeaker were made for two different input levels (1 and 4 V). Measurements were carried out using an exponential swept sine signal (from 50 Hz to 2 kHz) and the first five harmonics were separated using the technique described in Ref. [12]. Results are plotted in Fig. 3. The solid lines represent the measurement of the temporal evolution of the harmonics (fundamental frequency and harmonics due to distortion) while the dotted lines represent the same quantities calculated using the state-space model using the parameters

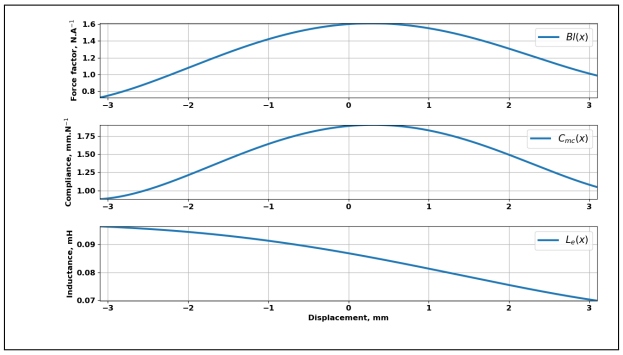

Figure 2. Dependence of the Bl factor (upper graph), compliance C_{mc}, (middle graph) and inductance L_e (lower graph) for one the loudspeaker units used in this work.

identified by the Klippel system. These parameters are listed in Table 1. Note that the resonance frequency of the closed-box system f_c is equal to 171.8 Hz.

For the 1 V input level, the amplitudes of the 2^{nd} and 3^{rd} order harmonics are somehow well predicted by the state space model for low frequencies. Above 400 Hz, the modeled 3^{rd} harmonic starts to attenuate much faster than that of the real loudspeaker. The 4^{th} and 5^{th} harmonics of the model do not represent the loudspeaker behaviour accurately, but this is certainly because these harmonics begin to be drowned out by the background noise at such low input level. For an input voltage of 4 V, the 2^{nd}, 3^{rd} and 5^{th} measured harmonics are close to the theoretical predictions up to 800 Hz while the amplitude of the 4^{th} one is underestimated. The results obtained here, although imperfect, are considered to be of reasonable quality and will be used later on to assess the effect of loudspeaker non-linearities in the context of sound zones.

Table 1. Loudspeaker parameters

Parameter	Value	Unit
R_e	4.15	Ω
L_e	0.091	mH
M_{ms}	0.48	g
C_{mc}	1.76	mm.N^{-1}
R_{ms}	0.193	kg.s^{-1}
Bl	1.3	N.A^{-1}
S_d	11	cm^2
f_c	171.8	Hz

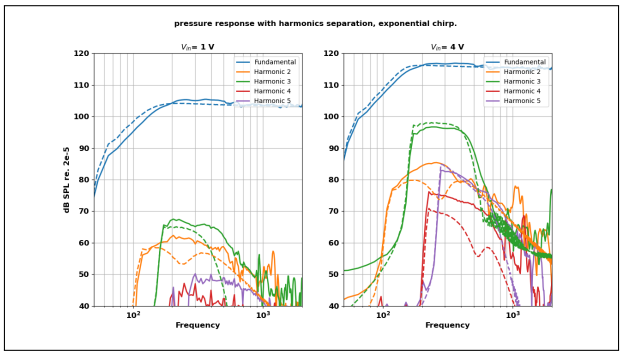

Figure 3. Pressure level radiated in the near field of a Tectonic loudspeaker: measurement (solid lines) and state-space model (dashed lines) of the higher harmonics frequency responses.

3. SOUND ZONE THEORY

The problem of interest consists in radiating an audio signal in a so-called bright zone while minimising it in a so-called dark zone by using an array of L loudspeakers. Each zone is sample by M microphone positions. The transfer function between a given loudspeaker l (with $l \in [1, L]$) and a given microphone m (with $m \in [1, M]$) is denoted $G_{b,d}(m, l)$, b and d respectively standing for bright and dark. Fig. 4 is showing the problem geometry. To ease the calculation, a matrix formalism is used here. Loudspeakers are then driven with voltage

$$\mathbf{u} = [1, \cdots, u_L]^T. \tag{9}$$

Pressure in the bright and dark zones are respectively denoted

$$\mathbf{p_b} = [p_b(1), \cdots, p_b(M)]^T, \tag{10}$$

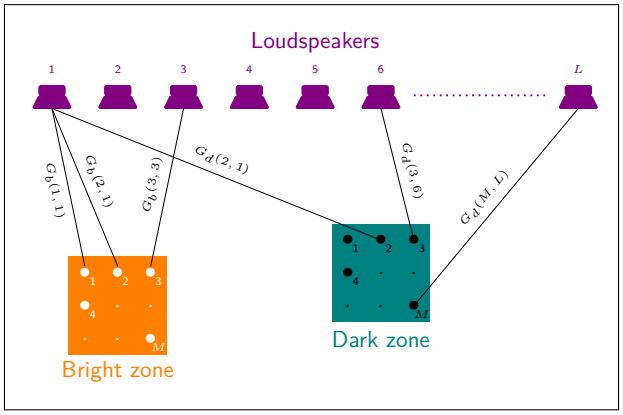

Figure 4. Geometry of interest.

and

$$\mathbf{p_d} = [p_d(1), \cdots, p_d(M)]^T. \tag{11}$$

They can be computed using the following equation

$$\mathbf{p_b} = \mathbf{G_b u} \text{ and } \mathbf{p_d} = \mathbf{G_d u}, \tag{12}$$

where matrices $\mathbf{G_b}$ and $\mathbf{G_d}$ are given by

$$\mathbf{G_{b,d}} = \begin{bmatrix} G_{b,d}(1,1) & \cdots & G_{b,d}(1,N) \\ \vdots & G_{b,d}(m,l) & \vdots \\ G_{b,d}(M,1) & \cdots & G_{b,d}(M,L) \end{bmatrix}. \tag{13}$$

Several algorithms have been proposed to calculated the input signals $\mathbf{u_f}$ that allows to meet the users' constraints. Here we have chosen to use the Weighted Pressure Matching (WPM) algorithm [4] which consists, in the following form, in minimising the following Lagrangian

$$\mathcal{L} = (1-\kappa)(\mathbf{p_b} - \mathbf{p_t})^H(\mathbf{p_b} - \mathbf{p_t}) + \kappa \mathbf{p_d}^H \mathbf{p_d} + \lambda \mathbf{u}^H \mathbf{u}, \tag{14}$$

where $0 < \kappa < 1$ is a parameter that allows to achieve a trade-off between the contrast and the reproduction error in the bright zone and λ is a regularization parameter that allows to control the speaker maximum input energy. The solution allows to radiate a pressure field in the bright zone close to the target $\mathbf{p_t}$ while minimizing the acoustic potential energy in the dark zone and the input signal energy. By differentiating the Lagrangian $\mathcal{L}$ with respect to the input voltage $\mathbf{u}$, we get

$$\mathbf{u} = [(1-\kappa)\mathbf{G_b}^H\mathbf{G_b} + \kappa \mathbf{G_d}^H \mathbf{G_d} + \lambda \mathbf{I}]^{-1}(1-\kappa)\mathbf{G_b}^H \mathbf{p_t}. \tag{15}$$

The performances of the WPM algorithm are evaluated using the following metrics:

- The contrast AC between the mean potential energy in the bright and dark zones is calculated using

$$AC = 10\log_{10}\left(\frac{\mathbf{p_b}^H\mathbf{p_b}}{\mathbf{p_d}^H\mathbf{p_d}}\right). \quad (16)$$

- The normalized mean square error E between the pressure in the bright zone $\mathbf{p_b}$ and the target pressure $\mathbf{p_t}$ is computed with

$$E = \frac{(\mathbf{p_t}-\mathbf{p_b})^H(\mathbf{p_t}-\mathbf{p_b})}{\mathbf{p_t}^H\mathbf{p_t}}. \quad (17)$$

These two metrics will be used hereafter to assess the effects of the speaker non-linearities on PSZ.

4. NUMERICAL SIMULATIONS

The WPM algorithm is now tested on a simplified automotive scenario. Two seats whose headrest are equipped with 4 loudspeakers are simulated (see Fig. 5). The source positions located on the x axis at $x_{sd} = [0.58, 0.505, 0.225, 0.15]$ for the DZ seat and $x_{sb} = -x_{sd}$ for the bright zone seat. The bright and dark zones areas are sampled by two regular grids of 3 by 3 microphones separated by $\Delta x = 2$ cm and $\Delta y = 5$ cm. The microphones marked with a black dot in Fig. 5 are located at $(-23.5, -1)$ cm and $(-45.5, -1)$ cm for the BZ and at $(23.5, -1)$ cm and $(45.5, -1)$ cm for the DZ. Please note that we consider here a free-field configuration: the diffraction on the seats and on the heads are not taken into account. The radiation of the sound sources is modelled using a point source approximation. The speaker volume velocities are calculated using the state space model presented in Sec. 2. Note that eight different loudspeakers were measured by the Klippel system in order to obtain 8 different sets of non-linear parameters and to more accurately represent the parameter variation that can exist between units in real life. The target pressure p_t is calculated by driving the two inner speakers of the bright zone seat with the same signal (mono configuration). For all simulations, $\kappa = 0.9$ and $\lambda = 10^{-6}$.

The contrast AC is plotted in Fig. 6 for several methods. The blue and orange curves are respectively computed with a Linear Parameter Model (LPM) using a Laplace filter and a linear state space representation (the effect of the reluctance force is removed and parameters Bl, C_{mc}, L_e are kept constant). One can see that the two curves are superimposed, which validates the coupling of the PM

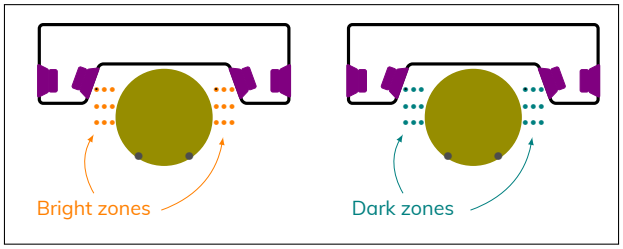

Figure 5. Simulation setup: a two car seat configuration with headrests equipped with four electrodynamic drivers.

algorithm with the state-space model. The AC exhibits a plateau value around 42 dB at low frequencies, then increases to a maximum value of 51 dB before decreasing to 33 dB around 1.2 kHz then increasing again.

Then, the non linear state space model is computed for several input levels of the swept sine signal (from 0.1 to 4 V). It can be seen that for an input voltage of 0.1 V, the linear and non-linear curves are not identical. Indeed, the linear parameters of the loudspeaker have been measured with the linear modulus of the Klippel system which assumes a linear behaviour of the loudspeaker, and thus represents a kind of average of these parameters. On the other hand, the non-linear parameters are measured for different input levels and are not necessarily optimal at low levels. It is therefore not surprising to obtain slightly different curves. As the input voltage is increased, the contrast drops for frequencies below 180 Hz, This decrease reaches 10 dB for an input level of 4 V. Between 180 Hz and about 500 Hz, strong oscillations of the contrast due to the non-linearities of the system can be observed.

In order to identify which parameters generate the most non-linearities, a parametric study was carried out. Thus all parameters depending on x are kept constant except one which uses the dependence measured in Section 2. The results are shown in Figure 7. First of all, it can be seen that the non-linearities due to the inductance have practically no effect on the frequency band considered. Indeed, the effect of the inductive reactance is negligible at low and medium frequencies compared to the value of the coil resistance. The curves also show that the non-linearities of the Bl factor or the suspension are quite close, the latter being however predominant from an excitation voltage of 2 V between 70 and 150 Hz. This can be explained by the fact that the displacement of the moving

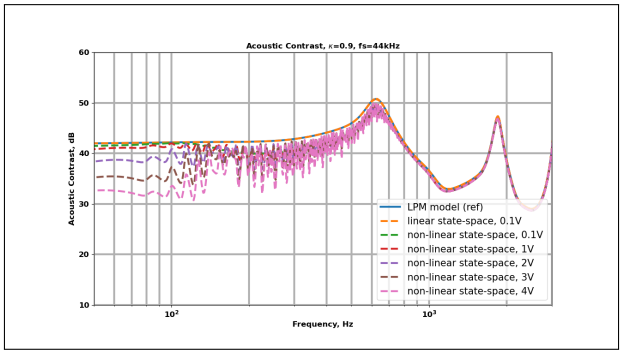

Figure 6. Contrast for different simulations: Linear Parameter Model (blue), linear state space model (orange), non-linear state space model for several input voltages (other colors).

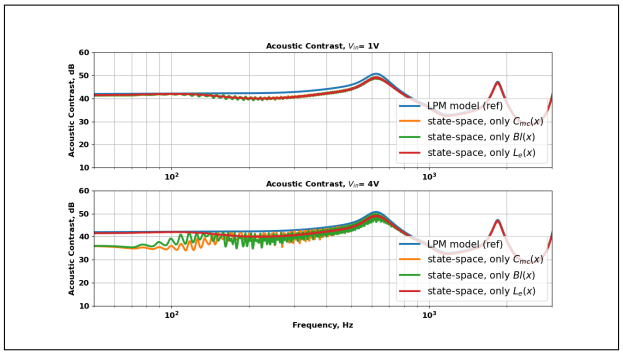

Figure 7. Parametric study highlighting the effect of Bl, C_{mc} and L_e on the contrast for four input levels (1 to 4 V).

part of the loudspeaker is maximum below the resonant frequency f_c where the restoring force of the suspensions is directly proportional to the diaphragm excursion.

Fig. 8 represents the normalised mean square error E computed with the linear state-space model for several sampling frequencies. It can be seen that for a sampling rate of 48 kHz, the discretization error is completely masking the error due to the PZS algorithm and which is why higher sampling rates are also tested. As the sampling rate is increased, the error obtained with the state-space model approaches that of the LPM simulation. An acceptable agreement between the results of the state space model and LPM is obtained for a sampling frequency of 1.536 MHz, the non-linear simulation was then run for different input levels using this sampling rate

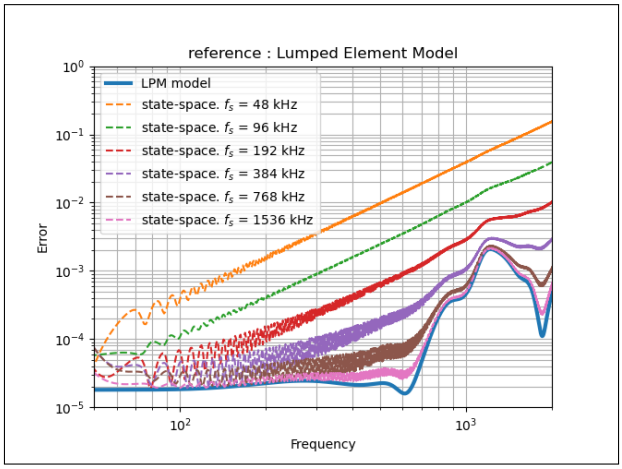

Figure 8. Normalized mean square error in the bright zones for different simulations: Linear Parameter Model (blue), linear state space model at different sampling rate (other colors)

value (see Fig. 9). At low frequencies, as the input voltage is increased, the error increases further from a plateau of about 2.10^{-5} to about 0.07. As already observed for the AC contrast, the error shows strong oscillations above 200 Hz. The effects of the loudspeaker non-linearities are visible up to about 1 kHz, beyond which value all curves almost merge.

5. MEASUREMENTS

Please note that these results were obtained under ideal conditions, i.e. without noise and with transfer functions calculated at the same positions. In general, to avoid what is known as inverse crime, the metrics are calculated at microphone positions slightly different from those used to calculate the filter, or with noise added. Here, the authors chose to assess the significance of the theoretical results by carrying out the following preliminary experiment. Two prototypes of headrests have been constructed, each incorporating four Tectonic TEBM35C10-4 speakers reproducing the configuration illustrated in Fig. 5. The microphoen grids used for the BZ and DZ remains consistent with that employed in the numerical simulation. Notably, the two Tectonic drivers situated in the center of the driver's headrest are positioned 5 cm lower than the line connecting the other six Tectonic drivers. Subsequently, the headrests are affixed to the front seats of two cars, alongside two artificial heads. The entire sys-

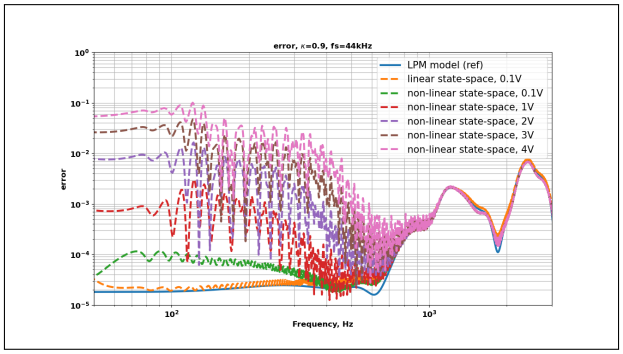

Figure 9. Normalized mean square error in the bright zones for different simulations: Linear Parameter Model (blue), linear state space model (orange), non-linear state space model for several input voltages (other colors)

tem is then installed within a semi-anechoic chamber (see Fig. 10). The filters were designed with transfer functions measured using a swept sinusoidal signal with a maximum amplitude of 1 V, while the contrast was evaluated with swept sinusoidal signals of 1, 2, 3 and 4 V. Results are shown in Fig. 11. The blue line represents the simulated contrast obtained under free-field conditions with monopolar sources. It follows the general trend observed with the measured data, with a few differences that may be due to noise, diffraction on speakers or dummy heads, or even speaker directivity. When we compare the curves obtained for the different excitation levels, we notice that the greatest differences are observed around the resonance frequency of the loudspeaker mounted on its closed load (between 100 and 200 Hz) where the contrast decreases as the input level increases. There are also fairly strong oscillations on the curves obtained with a 4 V signal. These results reproduce part of those obtained with the state-space model. However, a significant difference is observed below 100 Hz, where the expected drop in contrast with the input level is not found. This frequency band corresponds to a zone where the loudspeaker is no longer very effective, so it could be that the drop in contrast is masked by the increase in SNR when using the highest input levels.

6. CONCLUSION

In this paper, a state-space model has been used to predict the non-linear behaviour of electrodynamic speakers. This model was then tested on two-inch Tectonic drivers and

Figure 10. Experimental set-up.

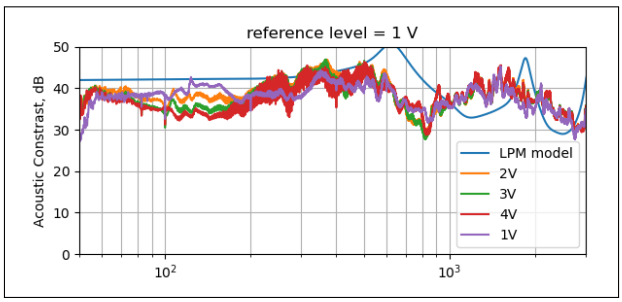

Figure 11. Comparison of the measured acoustic contrast with different input levels.

showed sufficient performance to be used in a personal sound zone scenario based on the WPM algorithm. The effect of the loudspeaker non-linearities was then assessed on the WPM results. The metrics considered (contrast AC and error E) were found to be significantly downgraded at low frequencies (up to 180 Hz for AC and 700 Hz for E), thus showing a substantial effect of the loudspeakers' non-linearities around their resonance frequency at high input levels.

Preliminary experimental results have been reported showing that some trends predicted with the state place model also occur in he experiment, but at a lower extent. However, further refined tests are still required to differentiate the impact of nonlinearities from those resulting from the signal-to-noise ratio.

In terms of future tasks, there are several avenues for enhancing the state space model, such as incorporating thermal effects. Another interesting direction would involve employing perceptual tests to establish acceptable thresholds for error and contrast degradation. This would enable optimal loudspeaker dimensioning based on the intended application. Additionally, leveraging the state space model during the filter design phase could yield more resilient filters. Investigating this aspect further holds promise for future research.

7. REFERENCES

[1] W. Druyvesteyn and J. Garas, "Personal sound," *Journal of the Audio Engineering Society*, vol. 45, no. 9, pp. 685–701, 1997.

[2] J.-W. Choi and Y.-H. Kim, "Generation of an acoustically bright zone with an illuminated region using multiple sources," *The Journal of the Acoustical Society of America*, vol. 111, no. 4, pp. 1695–1700, 2002.

[3] S. J. Elliott, J. Cheer, J.-W. Choi, and Y. Kim, "Robustness and regularization of personal audio systems," *IEEE Transactions on Audio, Speech, and Language Processing*, vol. 20, no. 7, pp. 2123–2133, 2012.

[4] J.-H. Chang and F. Jacobsen, "Sound field control with a circular double-layer array of loudspeakers," *The Journal of the Acoustical Society of America*, vol. 131, no. 6, pp. 4518–4525, 2012.

[5] W. Klippel, "Loudspeaker nonlinearities–causes, parameters, symptoms," in *Audio Engineering Society Convention 119*, (New York), Audio Engineering Society, 2005.

[6] X. Ma, P. J. Hegarty, J. A. Pedersen, L. G. Johansen, and J. J. Larsen, "Personal sound zones: The significance of loudspeaker driver nonlinear distortion," in *Audio Engineering Society Conference: 2016 AES International Conference on Sound Field Control*, Audio Engineering Society, 2016.

[7] X. Ma, P. J. Hegarty, J. A. Pedersen, L. G. Johansen, and J. J. Larsen, "Assessing the influence of loudspeaker driver nonlinear distortion on personal sound zones," in *Audio Engineering Society Convention 142*, (Berlin), Audio Engineering Society, 2017.

[8] N. Thiele, "Loudspeakers in vented boxes: Part 1," *Journal of the Audio Engineering Society*, vol. 19, no. 5, pp. 382–392, 1971.

[9] R. H. Small, "Closed-box loudspeaker systems-part 1: Analysis," *Journal of the Audio Engineering Society*, vol. 20, no. 10, pp. 798–808, 1972.

[10] D. Jakobsson and M. Larsson, *Modelling and compensation of nonlinear loudspeaker*. Master's Thesis, Chalmers University of Technology, 2010.

[11] P. Brunet, *Nonlinear system modeling and identification of loudspeakers*. PhD thesis, Northeastern University, 2014.

[12] A. Novak, P. Lotton, and L. Simon, "Synchronized swept-sine: Theory, application, and implementation," *Journal of the Audio Engineering Society*, vol. 63, no. 10, pp. 786–798, 2015.